

## Evidence for Rydberg Doorway States in Photoion Pair Formation in Bromomethane

Trevor Ridley,<sup>\*,†</sup> John T. Hennessy,<sup>†</sup> Robert J. Donovan,<sup>†</sup> Kenneth P. Lawley,<sup>†</sup> Shiliang Wang,<sup>‡,§</sup> Paul Brint,<sup>‡</sup> and Eoin Lane<sup>‡</sup>*School of Chemistry, The University of Edinburgh, West Mains Road, Edinburgh EH9 3JJ, Scotland, and Department of Chemistry, University College of Cork, Cork, Ireland**Received: January 9, 2008; Revised Manuscript Received: May 2, 2008*

The vacuum ultraviolet laser-excited photoion-pair formation spectrum of CH<sub>3</sub>Br has been measured under high resolution in the threshold region. The (2 + 1) and (3 + 1) resonance-enhanced multiphoton ionization spectra in the same energy region are also reported. By comparison of the spectra in this and a more extended region, resonances in the photoion-pair formation spectrum are assigned to p and f Rydberg states. It is concluded that all the structure in the photoion-pair formation spectrum near threshold can be accounted for by members of the  $\Omega = 0$  subset of Rydberg states that act as doorway states to the ion channel.

### I. Introduction

Three recent studies from different laboratories on photoion-pair formation in some halomethanes have been reported.<sup>1–3</sup> In two of these<sup>1,2</sup> it was concluded that the process was predominantly due to direct absorption into the ion-pair state continuum rather than via doorway Rydberg states that couple to this continuum. This is in contrast to our interpretation of the photoion-pair formation yield for some diatomic halogens, interhalogens, and hydrogen halides recorded as a function of excitation energy using both synchrotron<sup>4–7</sup> and vacuum ultraviolet (VUV) laser excitation.<sup>8</sup> All of the spectra were structured, and several Rydberg series were identified. The high-resolution VUV laser-excited spectra of I<sub>2</sub> and ICl were shown to closely follow the one-photon absorption cross-sections and no direct absorption to the free ion-pair continuum was observed. Hence it was concluded that all of the Rydberg states that are accessed act as efficient doorway states to ion-pair production in these diatomics. However, it was argued by Xu et al.<sup>1</sup> that their halomethane results cast some doubt on our interpretation of photoion production in diatomics. They suggested that the structure in their photoion-pair formation spectra was vibrational, arising from the difference in the geometry of the ground and ion-pair states.

To resolve the question of whether there really is a difference between the mechanism of photoion-pair production in the halomethanes and the diatomic halides, we reinvestigate this process in jet-cooled bromomethane (CH<sub>3</sub>Br) using some sets of data accumulated in our laboratory over recent years, namely, the VUV laser-excited photoion-pair formation spectrum in one narrow wavenumber region near the threshold for free-ion formation and a larger data set from (2 + 1) and (3 + 1) resonance-enhanced multiphoton ionization (REMPI) spectra up to the first ionization energy (IE). We use this extended data set as an aid to the classification of the states appearing in the ion-pair production spectrum. Propensity rules for one-, two-, and three-photon absorption will be proposed. From these, it

will be shown that the results of the earlier studies<sup>1–3</sup> are entirely consistent with the free ion-pairs being formed predominantly by absorption into Rydberg doorway states. The difference between the structure observed in the photoion-pair formation spectrum and that in the absorption spectrum is explained in terms of the different  $\Omega$  values of the Rydberg states that are dominant in the two experiments.

### II. Experimental Section

The molecular beam was generated by passing one atmosphere of pure CH<sub>3</sub>Br through a pulsed nozzle (General Valve, Iota One) with a 250- $\mu$ m diameter aperture, into the ionization region of a linear time-of-flight mass spectrometer. Ions were collected at 90° to both the molecular and laser beams. Mass-resolved ion signals (both positive and negative in the photoion-pair experiments) were processed by a Stanford Research SR250 boxcar integrator and stored on a PC.

The radiation in the REMPI experiments, provided by a Lambda Physik FL3002 dye laser pumped by a Lambda Physik EMG201MSC XeCl excimer laser, was focused by a 6 cm focal length lens into the interaction region with the molecular beam. The frequency-doubled outputs of the dyes RB, R6G, C153, C307, and C102 were used to record the (2 + 1) REMPI spectra and the fundamental outputs of C47, C120, S3, PBBO, QUI, and DMQ were used for the (3 + 1) REMPI spectra. In both experiments, circular polarization was achieved by passing the beam through a Soleilabinet prism. All (2 + 1) REMPI spectra were normalized to the square of the simultaneously recorded laser power. The laser wavelengths were calibrated using a combination of Br atomic lines and Ne optogalvanic lines.

The photoion-pair formation spectra were recorded using VUV laser radiation which was generated by four-wave difference frequency mixing in Kr gas. A Lambda Physik EMG201MSC XeCl excimer laser was used to pump two Lambda Physik dye lasers. The frequency doubled output of S3 provided a fixed frequency set to the two-photon resonance in Kr at 94094 cm<sup>-1</sup>. The third, tunable photon was provided by the fundamental of the dyes C153, R6G, RB, and R101. The VUV radiation was generated by combining the two beams collinearly and focusing them with a 20 cm focal length lens into a cell containing 10–20 Torr of Kr. The VUV output, covering the range 75700–78700 cm<sup>-1</sup> with a bandwidth of

\* To whom correspondence should be addressed. E-mail: T.Ridley@ed.ac.uk.

<sup>†</sup> The University of Edinburgh.

<sup>‡</sup> University College of Cork.

<sup>§</sup> Current address: DRDC Suffield, PO Box 4000, Station Main, Medicine Hat, Alberta, T1A 8K6 Canada.

$\sim 0.3 \text{ cm}^{-1}$ , was refocused, using a translatable 5 cm focal length LiF lens, into the pulsed molecular beam of CH<sub>3</sub>Br. In the present experiment, the visible and UV, as well as the VUV radiation, cross the molecular beam, which can result in a range of two-color excitation schemes. However, because of the widely different wavelengths of the three beams they have significantly different focal points, and it is possible, by careful positioning of both lenses, to selectively produce single photon VUV or VUV + UV/vis excitation. Only the former configuration was used in the present studies. The VUV was monitored by directing the beam exiting the ionization chamber, via an Acton Research Corporation VM-502 vacuum monochromator onto a Hamamatsu R1459 solar blind photomultiplier tube.

### III. The Classification and Assignment of Rydberg States of CH<sub>3</sub>Br

We will label the Rydberg states of CH<sub>3</sub>Br using the same description as that used<sup>9</sup> for Br<sub>2</sub> and the halogens in general. In the diatomic halogens,  $\Omega$ , the component of total electronic angular momentum about the internuclear axis,  $\mathbf{r}$ , is a good quantum number in Hund's cases a and c.  $\Omega$  is the sum of the axial component of the electronic angular momentum of the ionic core  $\Omega_c$  and that of the Rydberg electron  $\omega_{\text{Ryd}}$ .  $\omega_{\text{Ryd}}$ , in turn, is the sum of the axial component of the orbital angular momentum  $\lambda_{\text{Ryd}}$  and the spin  $m_s = \pm 1/2$  of the Rydberg electron.  $\Omega_c$  and  $\omega_{\text{Ryd}}$  together provide a useful basis set for the description of the lower Rydberg states. In this basis there is some mixing between states based on different values of  $\Omega_c$  but with the same  $\Omega$  and  $\lambda_{\text{Ryd}}$  values that arises from electron exchange between the core and Rydberg orbitals. In the limit when  $\Omega_c$  and  $\omega_{\text{Ryd}}$  are good quantum numbers, those states with a common  $\Omega$  value but different core states are of 1:1 singlet–triplet character. Thus, in the s series, only those states with  $\Omega = 1$  are of this mixed character, and in the p and higher series  $\Omega = 0$  states are among those of this mixed spin character. In the lower members of the p series, weak spin–orbit coupling in the Rydberg orbital, which must conserve  $\omega_{\text{Ryd}}$ , can also introduce mixed spin character into an apparently pure spin state. Thus, two closely spaced  $\Omega = 0$  states that will play a part in the following analysis of the spectra are the p states based on the  $^2\Pi_{1/2}$  state of the core. These must have  $|\omega_{\text{Ryd}}| = 1/2$  to create an  $\Omega = 0$  state, and the Rydberg spin–orbital is either  $\lambda = 1$ ,  $m_s = -1/2$  or  $\lambda = 0$ ,  $m_s = 1/2$ . The latter is apparently purely triplet in character because the spins in the core and Rydberg orbital are aligned parallel, but spin–orbit coupling mixes the two states and introduces some singlet character so that both become accessible in one-photon transitions from the singlet ground state.

The lowest ion-pair state in the hydrogen halides (in many ways the closest to the halomethanes) must have  $\Omega = 0$  and results from the promotion of a valence electron from the highest bonding  $\sigma$  orbital to the lowest antibonding  $\sigma^*$  orbital. This ion-pair state must also be a singlet state to correlate with two singlet ions,  $\text{H}^+ + \text{X}^-$ . The strongest ion-pair/Rydberg coupling is thus with Rydberg states having  $\Omega = 0$  and some singlet character. We propose the same propensity rule for the halomethanes.

Thus, the labeling scheme adopted here for Rydberg states is  $[\Omega_c]nl;\Omega$  where  $n$  is the principal quantum number of the Rydberg orbital. The spin–orbit coupling of the ionic core yields  $^2\Pi_{3/2}$  and  $^2\Pi_{1/2}$  states (using  $C_{\infty v}$  notation) which will be abbreviated to  $[^3/2]$  and  $[^1/2]$ . The reduction to  $C_{3v}$  symmetry means that a Rydberg electron moves in a potential that is not quite axially symmetric but contains a  $\cos 3\phi$  ripple, where  $\phi$

is the azimuthal angle about the top axis. This does not remove the degeneracy of  $\lambda_{\text{Ryd}} = 1$  or 2 states but does split the  $\lambda_{\text{Ryd}} = 3$  pair of states into an  $a_1$  and an  $a_2$  component. This first happens in the f series. The  $a_1$  component then mixes to some extent with any close-lying s state (for which  $\lambda_{\text{Ryd}} = 0$ ), which for both core states introduces some  $\Omega = 1$  character into what is nominally an  $\Omega = 2$  state and single-photon access that is dipole and spin allowed becomes possible in a perpendicular transition. However, we will not need to invoke  $\Omega = 1$  or  $\Omega = 2$  states in the following analysis and  $\Omega$  is treated as a good electronic quantum number.

The term values,  $T_{n,l} = \text{IE}(\Omega_c) - E_{n,l}$  of a Rydberg series converging on the state  $\Omega_c$  of the ion core for which the ionization energy is  $\text{IE}(\Omega_c)$ , are given to a good approximation by the formula

$$T_{n,l} = R/(n - \delta_l)^2 \quad (1)$$

where  $\delta_l$  is the quantum defect for the  $l$  series and the dependence of  $\delta_l$  on the state of the core and the remaining quantum numbers  $\lambda_{\text{Ry}}$  and  $\Omega$  has been omitted for brevity. The quantity that can be deduced directly from experimental term values is the effective principal quantum number,  $n^* = n - \delta_l$ . However, this step depends on using the correct IE for the series and an increasingly accurate value is needed as  $n$  increases in order to distinguish between series converging on the same limit.  $\delta_l$  can be found from  $n^*$  but only to modulo 1 because of the arbitrary choice of  $n$  that must be made for the first observed member of a series. For near-integer values this can lead to ambiguity; e.g.,  $n^* = 3.05$  cannot by itself distinguish between a 6s state with  $\delta = 2.95$  and a 4d state with  $\delta = 0.95$  and only if the first member of a series can be identified can this dilemma be resolved. The differentiation between p and f series is usually unambiguous because the latter will have  $n^*$  values, which are nearly integral, whereas in the former they will be approximately half-integral.

Recent ZEKE photoelectron studies<sup>10,11</sup> of CH<sub>3</sub>Br have determined values for the first IE ( $^2\Pi_{3/2}$ ) of  $85031.2 \pm 1 \text{ cm}^{-1}$  and for the second ( $^2\Pi_{1/2}$ ) of  $87615.2 \pm 4 \text{ cm}^{-1}$ . In the most recent analyses<sup>12,13</sup> of the VUV absorption spectrum of CH<sub>3</sub>Br, values of 85212 and 87930  $\text{cm}^{-1}$  were used for the two IEs. The large difference between these values and the true values obtained from the ZEKE study must lead to some uncertainty in the assignment of the higher- $n$  Rydberg states in the absorption spectrum. In the present study, the values obtained from the ZEKE study are used throughout.

In CH<sub>3</sub>Br, the lowest ion-pair state dissociates to  $\text{CH}_3^+(\text{X } ^1\text{A}_1) + \text{Br}^-(^1\text{S}_0)$ , so has  $\Omega = 0$ . We propose, as in the hydrogen halides, that the only Rydberg states that strongly couple with the ion-pair state, and thus act as doorway states to photoion production, are those with  $\Omega = 0$  and some singlet character. Therefore, the first aim of this study is to identify, using (2 + 1) and (3 + 1) REMPI spectra, as many  $\Omega = 0$  states as possible in the narrow wavenumber region where we have observed VUV laser-excited photoion-pair formation. Any  $\Omega = 0$  states observed in the (2 + 1) REMPI spectrum can be unambiguously identified from their polarization behavior.  $\Omega = 0$  and  $\Omega = 1$  states observed in the (3 + 1) REMPI spectrum cannot be differentiated from each other by their polarization behavior but can be distinguished from  $\Omega = 2$  and  $\Omega = 3$  states. We then compare the number of  $\Omega = 0$  states observed in the region of interest with the number that must exist in that range and see if these states, or a subset of them, are responsible for the structure in the one-photon photoion-pair formation spectra.

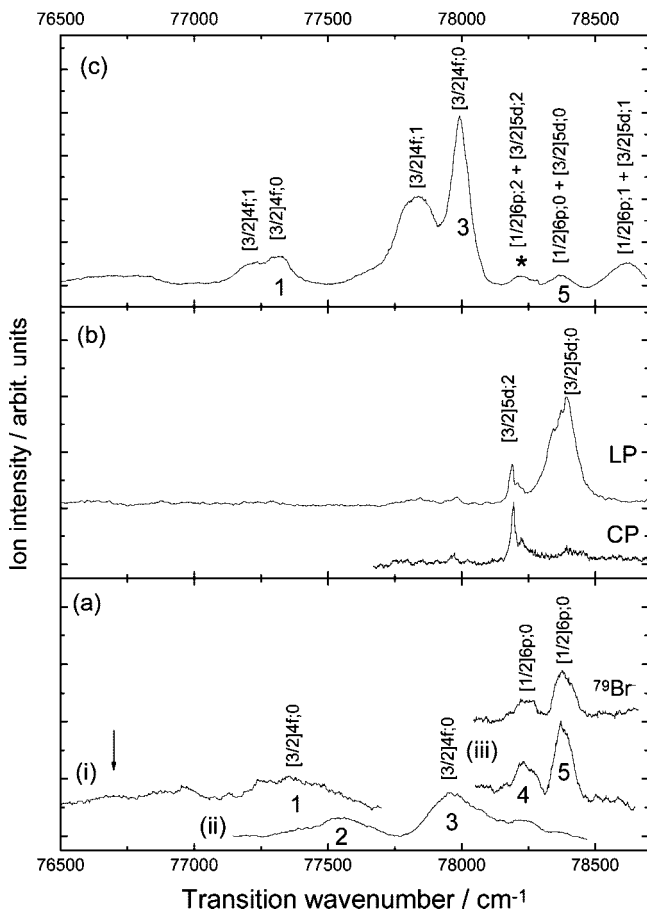


**Figure 1.** (a) The VUV laser-excited photoion-pair formation spectrum, (b) the (2 + 1) REMPI spectrum, and (c) the (3 + 1) REMPI spectrum of jet-cooled CH<sub>3</sub>Br over the range 76500–78700 cm<sup>-1</sup>. All spectra were recorded by collecting CH<sub>3</sub><sup>+</sup> with the exception of the upper trace of part a, section iii, which was recorded by collecting <sup>79</sup>Br<sup>-</sup>. In part a, sections i, ii, and iii were recorded by scanning the wavelength of the third photon over the lasing range of the dyes R6G, RB, and R101, respectively. In part b, the upper and lower traces show the spectra recorded with linearly polarized (LP) and circularly polarized (CP) light, respectively. The ion-pair formation threshold at 76695 cm<sup>-1</sup> is indicated by an arrow in part a.

#### IV. Results

**A. The VUV Laser-Excited Photoion-Pair Formation Spectrum.** The VUV laser-excited photoion-pair formation spectrum of jet-cooled CH<sub>3</sub>Br between 76500 and 78700 cm<sup>-1</sup> is shown in Figure 1a. The three sections of the spectra were recorded by scanning the wavelength of the tunable, third, photon over the range of the dyes, R6G (i), RB (ii), and R101 (iii). The spectra have not been power normalized and the baselines of the three sections have been offset for display purposes.

We attribute the spectrum purely to VUV photoion-pair formation rather than to a multiphoton process that also involves an additional UV/vis photon for three reasons. First, the spectra shown in sections i and ii and the lower trace of section iii were recorded by collecting CH<sub>3</sub><sup>+</sup>, but the same structure was observed, albeit more weakly, by collecting Br<sup>-</sup>. A small portion of the spectrum recorded by collecting <sup>79</sup>Br<sup>-</sup> is shown in the upper trace of (iii). We attribute this weaker negative ion signal, which is commonly observed in photoion-pair production below the first electronic IE, to a difference in detection efficiency. In any case, in CH<sub>3</sub>Br, the Br<sup>-</sup> signal would be half-that of CH<sub>3</sub><sup>+</sup> because the former is detected at mass 79, one of two equal

isotopic channels, but the latter appears in a single mass channel. Second, the wavenumber region down to 75700 cm<sup>-1</sup> was also generated by scanning the third photon over the range of the dye C153. However, no CH<sub>3</sub><sup>+</sup> signal was observed below the theoretical threshold for photoion-pair formation at 76695 cm<sup>-1</sup>, indicated by an arrow in Figure 1a, even though an intense band at 75822 cm<sup>-1</sup>, assigned to a [3/2]6p;0 Rydberg state, is observed in the VUV absorption spectrum. Third, structure in our spectrum corresponds to that excited by synchrotron radiation,<sup>2,3</sup> where two-photon processes can be ruled out.

Five peaks (bands 1–5), all of them quite broad, are observed at 77359, 77554, 77970, 78230, and 78390 cm<sup>-1</sup>. The first two combined correspond to the broad feature at 9.6 eV and the other three to the three-headed band centered at 9.7 eV in the synchrotron-excited absolute photoion-pair formation spectrum of Shaw et al.<sup>2</sup> The present spectrum is also generally consistent with a lower-resolution synchrotron-excited photoion-pair formation spectrum reported by Lochter et al.,<sup>3</sup> although the band positions appear to be offset by ~100 cm<sup>-1</sup>.

By use of the criterion of the effective quantum number,  $n^*$ , it is predicted that in all there are six  $\Omega = 0$  Rydberg states between 76500 and 78700 cm<sup>-1</sup>, namely, [3/2]5d (×2), [3/2]4f (×2), and [1/2]6p (×2). We will now try to identify some of these from the (2 + 1) and (3 + 1) REMPI spectra and see if their positions match those of the peaks in the photoion-pair formation spectrum. What follows is one particular set of assignments that are self-consistent and can explain the observations reported in previous photoion-pair formation spectra.<sup>1,2</sup>

**B. The (2 + 1) REMPI Spectrum.** The (2 + 1) REMPI spectrum of jet-cooled CH<sub>3</sub>Br between 65000 and 85000 cm<sup>-1</sup> is shown in Figure 2. The spectrum is a composite of several shorter scans each of which is normalized to the square of the laser intensity. These scans are then normalized to each other using the intensities of bands that are common to neighboring sections. However, some uncertainties in the relative intensities of the bands remain. The first IE at 85031 cm<sup>-1</sup> is indicated by an arrow.

Parent ions were never observed in the current REMPI experiments so the spectra were recorded by collecting CH<sub>3</sub><sup>+</sup> ions. The spectra could also be observed by collecting Br<sup>+</sup> ions, but these spectra were complicated by numerous (2 + 1) resonances in atomic bromine which did, however, provide convenient wavelength calibrations. The majority of the CH<sub>3</sub><sup>+</sup> and Br<sup>+</sup> almost certainly results from laser fragmentation of the parent ion. The band widths varied enormously between ~20 cm<sup>-1</sup>, e.g., the [3/2]5d;2 band, and ~200 cm<sup>-1</sup>, e.g., the [3/2]4d;0 band, and the uncertainties in the band positions vary correspondingly. The bandwidths will be discussed further in section V.

In assigning the two-photon spectrum of CH<sub>3</sub>Br the first comparison to be made is with the equivalent spectrum of Br<sub>2</sub>. In the centrosymmetric Br<sub>2</sub>, two-photon transitions from the gerade ground state are allowed only to the gerade  $ns$  and  $nd$  Rydberg states of the series that converge on the ground state of the ion. Although weak transitions to three of the four 5s states were observed, all of the remaining bands were assigned to  $nd$  states.<sup>9</sup> More specifically, four strong bands were observed in each  $nd$  cluster, [3/2] $nd$ ;2,0 and [1/2] $nd$ ;2,0. In each pair, the  $\Omega = 2$  band appeared at lower energy than the  $\Omega = 0$  band. In polarization experiments, the  $\Omega = 0$  bands were much weaker in the spectra recorded with CP light than in those recorded with LP light and were described as polarized bands. The remaining bands were more intense in the CP spectrum and

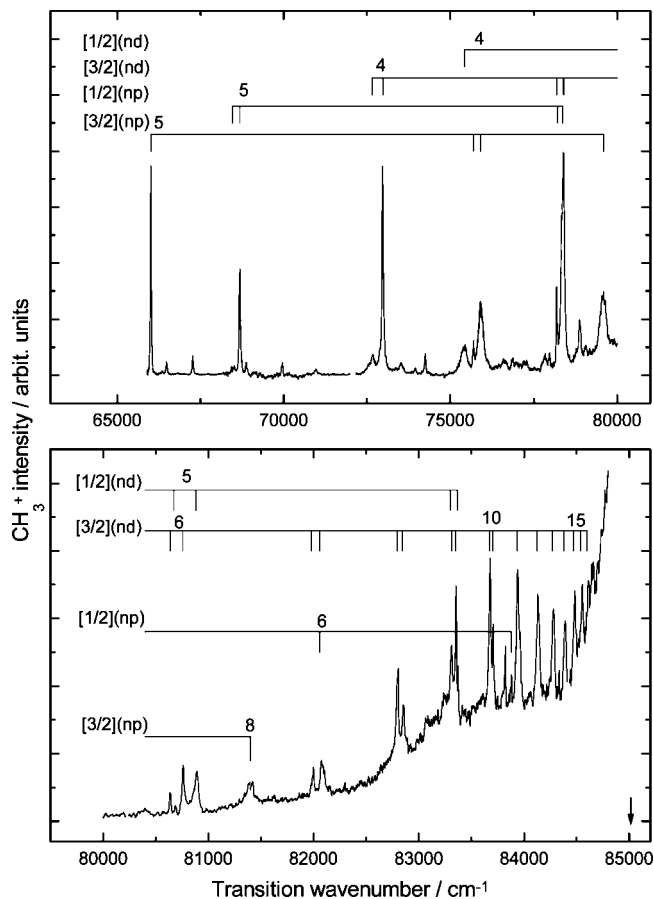


**Figure 2.** The power normalized (2 + 1) REMPI spectrum of jet-cooled CH<sub>3</sub>Br between 65000 and 85000 cm<sup>-1</sup> recorded with linearly polarized light. The first IE at 85031 cm<sup>-1</sup> is indicated by an arrow.

were said to be depolarized. Very few  $\Omega = 1$  bands were observed, and these were all very weak.

The analogous *nd* states are also observed in the (2 + 1) REMPI spectrum of CH<sub>3</sub>Br. Two *nd* series with ( $n = 4-16$ ) converging on the first IE are identified; for  $n \geq 11$ , the two states with a common  $n$  are not resolved. Two *nd* series with ( $n = 4-6$ ) converging on the second IE are also identified. Transitions to one *np* series converging on each of the two lowest IEs, with ( $n = 5-8$ ) and ( $n = 5-7$ ), respectively, are also observed. The analogous transitions to *np* states were not seen in the Br<sub>2</sub> spectrum as two-photon transitions from the gerade ground state to the ungerade *np* states are forbidden.

As in the Br<sub>2</sub> spectrum, the higher energy band of each pair that are assigned to *nd* states with a common  $n$  and ionic core is polarized, unambiguously labeling them as  $\Omega = 0$  states. Although polarization cannot distinguish between  $\Omega = 1$  and  $\Omega = 2$  states in two-photon spectra, by analogy with the Br<sub>2</sub> spectrum, the lower energy band of each pair is labeled as an  $\Omega = 2$  state. All of the observed *np* states are polarized, i.e., have  $\Omega = 0$ . The assignments, effective quantum numbers, and transition wavenumbers of the bands observed in the (2 + 1) REMPI spectrum are presented in Table 1.

**C. The (3 + 1) REMPI Spectrum.** The (3 + 1) REMPI spectrum of jet-cooled CH<sub>3</sub>Br between 65000 and 85000 cm<sup>-1</sup> is shown in Figure 3. No power normalization of these spectra was carried out. The intense broad band indicated by a star is due to (2 + 1) REMPI via the [3/2]5s;1 state.

The three-photon spectrum is dominated by transitions to *nf* Rydberg states: *nf* series with ( $n = 4-16$ ) and ( $n = 4-5$ ) converging on the first and second IEs, respectively, are

identified. The assignment to *nf* states is based on intensity arguments. As the cluster of bands around 78000 cm<sup>-1</sup> is approximately an order of magnitude more intense than that around 73000 cm<sup>-1</sup>, it is reasonable to assume that the former consists of the different  $\Omega$  components of the first member of a Rydberg series. By assumption that both clusters are due to Rydberg states with a <sup>2</sup> $\Pi_{3/2}$  ionic core, they have  $n^*$  values of  $\sim 4$  and  $\sim 3$ , respectively. It is only *nf* series whose first members have  $n^*$  values of  $\sim 4$ .

Transitions to the first member of all of the *nl* Rydberg series observed in the two-photon spectra are also observed here. While the 5p state bands are intense in both spectra, the 4d state bands that are intense in the two-photon spectrum are weak in the three-photon spectrum. With the exception of the weak band at 78229 cm<sup>-1</sup>, all of the bands are polarized indicating transitions to  $\Omega = 0$  or  $\Omega = 1$  states.

The assignments, effective quantum numbers and transition wavenumbers of the bands observed in the (3 + 1) REMPI spectrum are presented in Table 1. While the two-photon spectrum is quite sparse and the assignments appear reliable, the three- and one-photon spectra are more congested and consequently the assignments are less certain. For example, in the three-photon spectrum the higher energy band of each pair of bands that are assigned to *nd*;1 states based on either ionic core can equally well be assigned to an ( $n + 2$ );1 state based on the same core.

**D. The One-Photon Absorption Spectrum.** The band positions and intensity trends observed in the two- and three-photon spectra can throw new light on the analysis of the one-photon absorption spectrum, which in turn is required to interpret the photoion-pair formation spectrum. The VUV absorption spectrum has been widely studied using various excitation sources.<sup>12-15</sup> The positions reported by Causley and Russell<sup>15</sup> and Baig et al.<sup>12</sup> for bands below and above 84000 cm<sup>-1</sup>, respectively, are also presented in Table 1.

The reported analyses of the absorption spectrum all agree on the assignment of one *np* series converging on each of the first two IEs. However, the remainder of the spectrum has been assigned to varying combinations of *ns*, *nd*, and *nf* states.<sup>12-15</sup> We propose that of the *ns* and *nd* states only one  $\Omega = 1$  component of the 5s and 4d states based on each ionic core is observed with significant intensity and that all of the remaining structure consists of *nf* states. The assignment of the *np* series remains valid.

In summary, different propensities are observed for one-, two-, and three-photon transitions in CH<sub>3</sub>Br in addition to the normal selection rules. In all three types of spectra, transitions to the lowest members of all *nl* Rydberg series are observed. As  $n$  increases, there are propensities for transitions to particular *nl* series to dominate in the different multiphoton spectra: *np* and *nf* states in one-photon, *nd* states in two-photon, and *nf* states in three-photon. These propensities are now used to identify the states observed in the region in which the VUV laser-excited photoion-pair formation spectrum has been recorded.

**E. Detailed Assignment of the 76500–78700 cm<sup>-1</sup> Region.**

By use of the criterion of the effective quantum number,  $n^*$ , it is predicted that the [3/2]7s, [3/2]5d, [3/2]4f, and [1/2]6p Rydberg states lie in this region. There are allowed one-photon transitions to 16 of these states of which six have  $\Omega = 0$ , namely, [3/2]5d ( $\times 2$ ), [3/2]4f ( $\times 2$ ), and [1/2]6p ( $\times 2$ ). Furthermore, the propensities predict that only the [3/2]4f and [1/2]6p states should appear with appreciable intensity in the one-photon spectrum. To assign the one-photon bands we first examine the three-photon

**TABLE 1: Assignments, Effective Quantum Numbers ( $n^*$ ), and Transition Wavenumbers of the Bands Observed in the One-, Two-, and Three-Photon Spectra of  $\text{CH}_3\text{Br}^a$** 

assignment $[\text{P}_{3/2,1/2}]nl;\omega$	$n^*$	1-photon transition wavenumber/ $\text{cm}^{-1}$	2-photon transition wavenumber/ $\text{cm}^{-1}$	3-photon transition wavenumber/ $\text{cm}^{-1}$
$[\text{P}_{3/2}]5p;0$	2.40	66003 <sup>b</sup>	66019 <sup>d</sup>	66037
$[\text{P}_{3/2}]5p;1$	2.50			67445
$[\text{P}_{1/2}]5p;2$	2.39		68461	
$[\text{P}_{1/2}]5p;0$	2.41	68659 <sup>b</sup>	68684 <sup>d</sup>	68695
$[\text{P}_{1/2}]5p;1+$	2.50	70083 <sup>b</sup>		70102
$[\text{P}_{3/2}]4d;1$	2.71	70083 <sup>b</sup>		
$[\text{P}_{3/2}]4d;2$	2.98		72655	
$[\text{P}_{1/2}]4d;1$	2.74	72957 <sup>b</sup>		
$[\text{P}_{3/2}]4d;0$	3.02		72977 <sup>d</sup>	72968
$[\text{P}_{3/2}]4d;1$	3.10			73615
$[\text{P}_{1/2}]4d;0$	3.00		75418 <sup>d</sup>	75416
$[\text{P}_{3/2}]6p;2$	3.43		75686	
$[\text{P}_{3/2}]6p;0$	3.47	75822 <sup>b</sup>	75905 <sup>d</sup>	75897
$[\text{P}_{3/2}]6p;1+$	3.51			76124
$[\text{P}_{1/2}]4d;1$	3.10			76124
$[\text{P}_{3/2}]4f;1$	3.74			77197
$[\text{P}_{3/2}]4f;0$	3.77			77324
$[\text{P}_{3/2}]4f;1$	3.90	77871 <sup>b</sup>		77840
$[\text{P}_{3/2}]4f;0$	3.95			77993
$[\text{P}_{3/2}]5d;2$	4.01		78193	
$[\text{P}_{1/2}]6p;2$	3.42		78225	78229
$[\text{P}_{1/2}]6p;0$	3.45	78372 <sup>b</sup>	78370 <sup>d</sup>	78376
$[\text{P}_{3/2}]5d;0$	4.07		78401 <sup>d</sup>	
$[\text{P}_{3/2}]5d;1+$	4.14			78638
$[\text{P}_{1/2}]6p;1$	3.50			78638
$[\text{P}_{3/2}]7p;0$	4.50	79544 <sup>b</sup>	79610 <sup>d</sup>	
$[\text{P}_{1/2}]4f;1$	3.77			79905
$[\text{P}_{1/2}]4f;0$	3.81			80071
$[\text{P}_{3/2}]5f;1/0$	4.79			80249
$[\text{P}_{1/2}]4f;1$	3.90	80427 <sup>b</sup>		80416
$[\text{P}_{1/2}]4f;0+$	3.94	80511 <sup>b</sup>		80557
$[\text{P}_{3/2}]5f;1/0$	4.95	80511 <sup>b</sup>		80557
$[\text{P}_{3/2}]6d;2$	5.00		80640	
$[\text{P}_{1/2}]5d;2$	3.98		80674	
$[\text{P}_{3/2}]6d;0$	5.07		80758 <sup>d</sup>	80787
$[\text{P}_{1/2}]5d;0$	4.03		80881 <sup>d</sup>	80906
$[\text{P}_{1/2}]5d;1$	4.10			81158
$[\text{P}_{3/2}]8p;0$	5.48	81257 <sup>b</sup>	81375 <sup>d</sup>	
$[\text{P}_{3/2}]6f;1/0$	5.79			81760
$[\text{P}_{3/2}]6f;1/0$	5.94	81869 <sup>b</sup>		81916
$[\text{P}_{3/2}]7d;2$	6.00		81980	
$[\text{P}_{1/2}]6p;0+$	4.44	82050 <sup>b</sup>	82057 <sup>d</sup>	
$[\text{P}_{3/2}]7d;0$	6.07		82057 <sup>d</sup>	82069
$[\text{P}_{3/2}]7d;1$	6.16			82137
$[\text{P}_{3/2}]9p;0$	6.45	82395 <sup>b</sup>		
$[\text{P}_{3/2}]7f;1/0$	6.90	82715 <sup>b</sup>		82723
$[\text{P}_{3/2}]8d;2$	7.01		82795	
$[\text{P}_{3/2}]8d;0$	7.09		82846 <sup>d</sup>	
$[\text{P}_{1/2}]5f;1/0$	4.87	82997 <sup>b</sup>		82998
$[\text{P}_{3/2}]10p;0$	7.35	82997 <sup>b</sup>		
$[\text{P}_{1/2}]5f;1/0$	4.93			83112
$[\text{P}_{3/2}]8f;1/0$	7.95	83266 <sup>b</sup>		83293
$[\text{P}_{1/2}]6d;2$	5.04		83298	
$[\text{P}_{3/2}]9d;2$	7.99		83310	
$[\text{P}_{3/2}]9d;0$	8.08		83351 <sup>d</sup>	
$[\text{P}_{1/2}]6d;0$	5.08		83370 <sup>d</sup>	
$[\text{P}_{3/2}]9f;1/0$	8.92	83621 <sup>b</sup>		83653
$[\text{P}_{3/2}]10d;2$	8.98		83669	
$[\text{P}_{3/2}]10d;0$	9.09		83704 <sup>d</sup>	
$[\text{P}_{1/2}]7p;0$	5.43	83888 <sup>b</sup>	83879 <sup>d</sup>	
$[\text{P}_{3/2}]11d;2,0$	10.00		83934	
$[\text{P}_{3/2}]10f;1/0$	10.05	83899 <sup>c</sup>		83945
$[\text{P}_{3/2}]11f;1/0$	10.84	84097 <sup>c</sup>		---
$[\text{P}_{3/2}]12d;2,0$	10.99		84122	
$[\text{P}_{3/2}]12f;1/0$	11.86	84244 <sup>c</sup>		84251
$[\text{P}_{3/2}]13d;2,0$	12.01		84270	
$[\text{P}_{3/2}]13f;1/0$	12.89	84364 <sup>c</sup>		84371
$[\text{P}_{3/2}]14d;2,0$	12.96		84378	
$[\text{P}_{3/2}]14f;1/0$	14.06	84454 <sup>c</sup>		84476
$[\text{P}_{3/2}]15d;2,0$	14.00		84471	
$[\text{P}_{3/2}]15f;1/0$	14.90	84525 <sup>c</sup>		84537
$[\text{P}_{3/2}]16d;2,0$	14.92		84538	
$[\text{P}_{3/2}]16f;1/0$	15.77	84585 <sup>c</sup>		84590
$[\text{P}_{3/2}]17d;2,0$	15.94		84599	

<sup>a</sup> The effective quantum numbers are calculated using IEs of 85031 and 87615  $\text{cm}^{-1}$ .<sup>10,11</sup> <sup>b</sup> Causley and Russell.<sup>15</sup> <sup>c</sup> Baig et al.<sup>12</sup>  
<sup>d</sup> Polarized band.

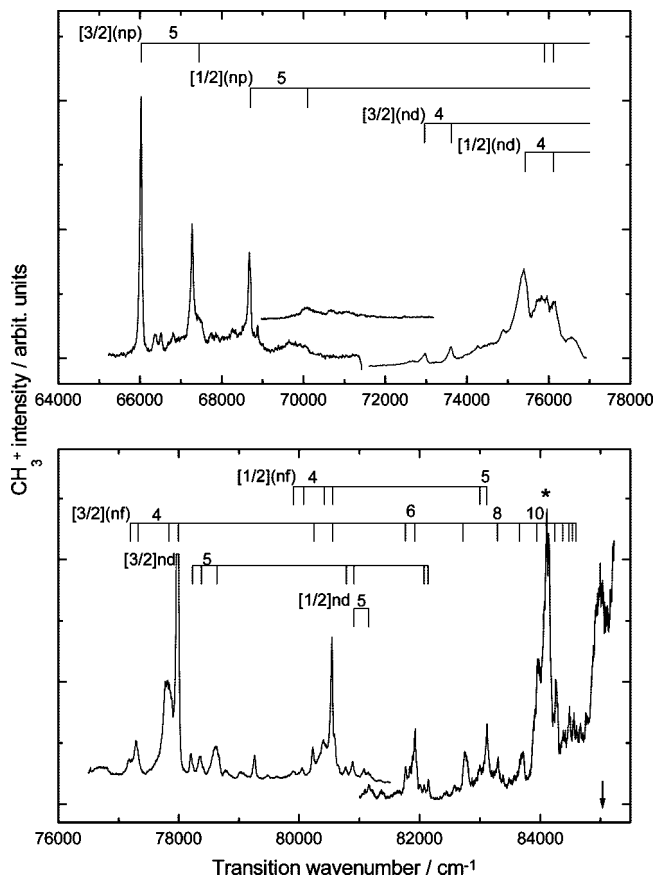


**Figure 3.** The (3 + 1) REMPI spectrum of jet-cooled  $\text{CH}_3\text{Br}$  between 65000 and 85000  $\text{cm}^{-1}$  recorded with linearly polarized light. The first IE at 85031  $\text{cm}^{-1}$  is indicated by an arrow.

spectrum since the propensities predict that the one- and three-photon spectra should be similar.

The VUV laser-excited photoion-pair formation spectrum, the (2 + 1) and (3 + 1) REMPI spectra over the range 76500–78700  $\text{cm}^{-1}$ , are shown in parts a, b, and c of Figure 1, respectively. Seven bands can be immediately identified in the (3 + 1) REMPI spectra shown Figure 1c. The polarization behavior indicates that, with the exception of the weak band indicated by a star, all of the bands are due, at least in part, to  $\Omega = 0$  or  $\Omega = 1$  states.

We are now in a position to assign the portion of the VUV laser-excited photoion-pair formation spectrum shown in Figure 1a. Bands 1, 3, and 5 can be assigned as  $[\text{P}_{3/2}]4f;0$ ,  $[\text{P}_{3/2}]4f;0$ , and  $[\text{P}_{1/2}]6p;0$  bands, i.e., those observed at 77324, 77993, and 78376  $\text{cm}^{-1}$  in the three-photon spectrum. Band 4 can be assigned as the second  $[\text{P}_{1/2}]6p;0$  state that is too weak to be seen in the three-photon spectrum. It is seen in the one-photon spectrum because the propensity for transitions to  $np$  states in one-photon spectra is greater than in three-photon spectra. The two  $[\text{P}_{3/2}]5d$  states are probably not seen in the photoion-pair formation spectrum although the one that appears very strongly in the two-photon spectrum may make a weak contribution to band 4. We tentatively assign band 2, together with the very weak broad signal between the ion-pair formation threshold and band 1, to vibronic structure associated chiefly with the  $[\text{P}_{3/2}]6p;0$  state whose origin at 75822  $\text{cm}^{-1}$  lies below the threshold for free ion-pair production and thus requires vibrational assistance.

The assignments of the bands observed in the spectra shown in Figure 1 are presented in Table 2. In general, we propose that the photoion-pair formation spectrum of  $\text{CH}_3\text{Br}$  is comprised

**TABLE 2: Assignments and Transition Wavenumbers of the Bands Observed in the Photoion-Pair Formation and Two- and Three-Photon REMPI Spectra of CH<sub>3</sub>Br in the Range 77000–79000 cm<sup>-1</sup>**

assignment [ <sup>2</sup> Π <sub>3/2,1/2</sub> ]nl;ω	1-photon transition wavenumber/ cm <sup>-1</sup>	1-photon transition wavenumber <sup>a</sup> / cm <sup>-1</sup>	2-photon transition wavenumber/ cm <sup>-1</sup>	3-photon transition wavenumber/ cm <sup>-1</sup>
[ <sup>3</sup> / <sub>2</sub> ]4f;1	77359	77340		77197
[ <sup>3</sup> / <sub>2</sub> ]4f;0	77554	77590		77324
[ <sup>3</sup> / <sub>2</sub> ]4f;1				77840
[ <sup>3</sup> / <sub>2</sub> ]4f;0	77970	77993	77973	77993
[ <sup>3</sup> / <sub>2</sub> ]5d;2			78193	
[ <sup>1</sup> / <sub>2</sub> ]6p;0	78230	78235		
[ <sup>1</sup> / <sub>2</sub> ]6p;2			78225	78229
[ <sup>1</sup> / <sub>2</sub> ]6p;0	78390	78397	78370	78376
[ <sup>3</sup> / <sub>2</sub> ]5d;0			78401	
[ <sup>3</sup> / <sub>2</sub> ]4f;1				78638

<sup>a</sup> Estimated from Figure 3c of ref 2.

of the  $\Omega = 0$  components of the [<sup>3</sup>/<sub>2</sub>,<sup>1</sup>/<sub>2</sub>]np and nf Rydberg states whereas the absorption spectrum in the same region is comprised of both  $\Omega = 0$  and  $\Omega = 1$  components.

## V. Discussion

Xu et al.<sup>1</sup> recorded the VUV laser-excited photoion-pair formation spectrum and photofragment images of CH<sub>3</sub>Br in the range 122.7–121.2 nm (81500–82508 cm<sup>-1</sup>). From the results of both studies they concluded that the ion-pair state continuum was being directly excited. However, we believe that their results are also explained by our proposed mechanism, in which the ion-pair state continuum is accessed via  $\Omega = 0$  Rydberg states.

In their photoion-pair formation spectrum Xu et al.<sup>1</sup> observed three bands at 81678, 81860, and 82062 cm<sup>-1</sup> that can now be assigned as two [<sup>3</sup>/<sub>2</sub>]6f;0 states and one [<sup>3</sup>/<sub>1</sub>]7p;0 state, respectively. The authors reported that the photoion-pair formation spectrum closely followed the absorption spectrum in the region that they investigated although detailed comparison was impossible because there was no comparable high-resolution absorption spectrum. We propose that there really are significant differences between the two spectra as described above but that these are not detectable because of the low resolution of the absorption spectrum.

The same authors also recorded photofragment images following excitation at five wavelengths, three on-resonance and two off-resonance with peaks in their photoion-pair formation spectrum. As the  $\beta$  parameters obtained at all five wavelengths were the same, they again concluded that the ion-pair state continuum was being directly excited. At the three on-resonance wavelengths the authors believed that both  $\Omega = 0$  and  $\Omega = 1$  states (in our description) were being excited; hence they expected to see different photodissociation dynamics when the different Rydberg states were excited but no such differences were observed. Again, we propose that resonances in the photoion-pair formation spectrum are due only to  $\Omega = 0$  states.

The question then arises of which  $\Omega = 0$  Rydberg states could be weakly excited at the off-resonance wavelengths. First, there are the origins of a second [<sup>1</sup>/<sub>2</sub>]7p state and two [<sup>3</sup>/<sub>2</sub>]7d states. Second, there is vibronic structure associated with the strong lower-energy  $\Omega = 0$  electronic origins. All of these bands will have similar bandwidths of  $\sim 70$  cm<sup>-1</sup> and will overlap to produce a pseudocontinuum of  $\Omega = 0$  Rydberg doorway states. The possibility still remains, of course, that the off-resonance ion-pair production is due, in part, to direct absorption into the ion-pair continuum. Conversely, it is difficult to explain why

direct absorption into the ion-pair continuum would produce such a structured photoion-pair formation spectrum.

Finally, Xu et al.<sup>1</sup> contrasted the results of their photofragment imaging studies on CH<sub>3</sub>Br, in which the  $\beta$  parameter remained constant with wavelength, with those of Li et al.<sup>16</sup> on CH<sub>3</sub>F in which the  $\beta$  parameter varied significantly with wavelength. Since Li et al.<sup>16</sup> modeled their results using a mechanism that involved doorway Rydberg states, Xu et al.<sup>1</sup> concluded that their mechanism did not involve doorway Rydberg states. However, the excitations in the two molecules are not to equivalent energy regions and hence the mechanisms for ion-pair formation are not directly comparable. In the CH<sub>3</sub>F studies<sup>16</sup> the molecule is excited to energies well above the first IE, and the proposed mechanism involves the initial excitation of Rydberg states converging on excited states of the parent ion. The mechanism proceeds via internal conversion to highly vibrationally excited levels of Rydberg states converging on the ground-state of the ion and thence to the ion-pair continuum. In the CH<sub>3</sub>Br studies, the molecule is excited to energies below the first IE, and the proposed mechanism involves initial excitation of Rydberg states converging on the ground-state of the parent ion and thence to the ion-pair continuum. If the time scale for the ion-pair formation, and hence the  $\beta$  parameter, is dictated in CH<sub>3</sub>F by the Rydberg-to-Rydberg transition, rather than the Rydberg-to-ion-pair continuum transition in CH<sub>3</sub>Br, then the photofragment imaging results may well be very different in the two studies.

Shaw et al.<sup>2</sup> recorded the synchrotron-excited photoion-pair formation and absorption spectra of CH<sub>3</sub>Br over the range 132–118 nm (75760–84750 cm<sup>-1</sup>). They reported that in the region between threshold and 80250 cm<sup>-1</sup> there was little correlation between the peaks in the two spectra. It was argued that photoion-pair formation resulted from direct absorption into the ion-pair continuum because peaks in the ion production channel did not correspond to intense features in the absorption spectrum.

We believe that our proposed mechanism can also explain these observations. A peak in their photoion-pair formation spectrum always coincides with a significant though not necessarily a major feature in the absorption spectrum. As above, we propose that the difference between the two spectra is that the absorption spectrum contains  $\Omega = 0$  and  $\Omega = 1$  bands, whereas the photoion-pair formation spectrum only contains  $\Omega = 0$  bands. For example, the intense absorption band estimated from their Figure 3a to lie at 9.67 eV (77993 cm<sup>-1</sup>) is comprised of [<sup>3</sup>/<sub>2</sub>]4f;1 and [<sup>3</sup>/<sub>2</sub>]4f;0 components which are unresolved with synchrotron resolution but which are resolved in the (3 + 1) REMPI spectrum shown in Figure 1c. Only the latter component appears in the photoion-pair formation spectrum, band 3 in Figure 1a. By contrast, bands 4 (9.70 eV) and 5 (9.72 eV), both [<sup>1</sup>/<sub>2</sub>]6p;0 bands, are not overlapped by any  $\Omega = 1$  bands in the absorption spectrum, even with synchrotron resolution. Hence, the intensities of the 9.70- and 9.72-eV bands relative to that of the 9.67-eV band are greater in the synchrotron-excited photoion-pair formation spectrum than they are in the equivalent absorption spectrum.

In the region between threshold and 80250 cm<sup>-1</sup>, each absorption band, with synchrotron resolution, contains a different percentage contribution from  $\Omega = 0$  and  $\Omega = 1$  states and hence the relative intensities of the bands in the two spectra are very different. As the wavenumber increases, the spectra become more congested and each absorption band contains an increasingly similar percentage contribution from  $\Omega = 0$  and  $\Omega = 1$  states and hence the relative intensities of the bands in the two

spectra become increasingly similar, as can be seen from Figure 3 of ref 2.

Shaw et al.<sup>2</sup> observed that the photoion-pair formation efficiency of CH<sub>3</sub>Br has a sharp onset at threshold and gradually increases as the transition wavenumber increases. This suggests that the strength of the coupling between the ion-pair state and the Rydberg doorway states increases likewise. In contrast, in CH<sub>3</sub>Cl, the photoion-pair efficiency had no obvious sharp onset at threshold and only begins to increase appreciably  $\sim 4000\text{ cm}^{-1}$  above threshold. Thus, it appears that the coupling between the ion-pair state and the electronic origins of the Rydberg doorway states in CH<sub>3</sub>Cl only begins well above threshold. It is possible that coupling between the ion-pair state and the Rydberg doorway states with some vibrational modes excited does occur in this  $4000\text{-cm}^{-1}$  region.

Since coupling between the ion-pair state and  $\Omega = 0$  Rydberg states occurs at threshold in CH<sub>3</sub>Br, it must continue over a certain range below threshold. This coupling will not result in photoion-pair formation but will produce a very dense manifold of vibronic levels with mixed Rydberg/ion-pair character centered on the position of the uncoupled Rydberg level. We would expect these coupled levels to be unresolvable and for them to appear as a single broad band. The band widths observed in the (2 + 1) REMPI appear to support this expectation. The widths of the two bands nearest to, but below, threshold, namely, the  $[^3/2]6p;0$  ( $75889\text{ cm}^{-1}$ ) and  $[^1/2]4d;0$  ( $75418\text{ cm}^{-1}$ ) bands, have widths of  $\sim 200\text{ cm}^{-1}$ , while the  $[^3/2]4d;0$  ( $72977\text{ cm}^{-1}$ ) and  $[^1/2]5p;0$  ( $68674\text{ cm}^{-1}$ ) both have band widths of only  $\sim 50\text{ cm}^{-1}$ .

## VI. Conclusions

By use of data from more extended 2- and 3-photon REMPI spectra, we have assigned the spectroscopic character of the transitions observed in the 1-photon absorption spectrum of CH<sub>3</sub>Br. By comparison of the structure in the absorption spectrum in the threshold region for ion-pair production with the structure in the photoion-pair production spectrum, we have

assigned the latter almost entirely to  $\Omega = 0$  Rydberg states based on the lower members of the p and f series. A relatively small amount of broad, unstructured direct absorption into the ion-pair continuum may underlie this structure. These doorway Rydberg states may not be particularly prominent in the 1-photon absorption spectrum, but they are dominant in photoion-pair formation, which is sensitive to this type of homogeneous coupling.

**Acknowledgment.** We thank the University of Edinburgh for a Scholarship and the CVCP for an ORS award for S.W.

## References and Notes

- (1) Xu, D.; Huang, J.; Price, R. J.; Jackson, W. M. *J. Phys. Chem. A* **2004**, *108*, 9916.
- (2) Shaw, D. A.; Holland, D. M. P.; Walker, I. C. *J. Phys. B: At. Mol. Opt. Phys.* **2006**, *39*, 3549.
- (3) Loch, R.; Leyh, B.; Dehareng, D.; Hottmann, K.; Jochims, H. W.; Baumgärtel, H. *Chem. Phys.* **2006**, *323*, 458.
- (4) Yench, A. J.; Kela, D. K.; Donovan, R. J.; Hopkirk, A.; Kvaran, A. *Chem. Phys. Lett.* **1990**, *165*, 283.
- (5) Kvaran, A.; Yench, A. J.; Kela, D. K.; Donovan, R. J.; Hopkirk, A. *Chem. Phys. Lett.* **1991**, *179*, 263.
- (6) Kaur, D.; Yench, A. J.; Donovan, R. J.; Kvaran, A.; Hopkirk, A. *Org. Mass. Spectrom.* **1993**, *28*, 327.
- (7) Yench, A. J.; Kaur, D.; Donovan, R. J.; Kvaran, A.; Hopkirk, A.; Lefebvre-Brion, H.; Keller, F. *J. Chem. Phys.* **1993**, *99*, 4986.
- (8) Lawley, K. P.; Flexen, A. C.; Maier, R. R. J.; Manck, A.; Ridley, T.; Donovan, R. J. *Phys. Chem. Chem. Phys.* **2002**, *4*, 1412.
- (9) Donovan, R. J.; Flexen, A. C.; Lawley, K. P.; Ridley, T. *Chem. Phys.* **1998**, *226*, 217.
- (10) Shi, Y. J.; Wang, S.; Jakubek, Z. J.; Simard, B. *Can. J. Chem.* **2004**, *82*, 1077.
- (11) Urban, B.; Bondybey, V. E. *J. Chem. Phys.* **2002**, *116*, 4938.
- (12) Baig, M. A.; Connerade, J. P.; Holmes, J. *J. Phys. B: At. Mol. Phys.* **1982**, *15*, L5.
- (13) Loch, R.; Leyh, B.; Jochims, H. W.; Baumgärtel, H. *Chem. Phys.* **2005**, *317*, 73.
- (14) Loch, R.; Leyh, B.; Dehareng, D.; Jochims, H. W.; Baumgärtel, H. *Chem. Phys.* **2005**, *317*, 87.
- (15) Causley, G. C.; Russell, B. R. *J. Chem. Phys.* **1975**, *62*, 848.
- (16) Li, W.; Lucchese, R. R.; Doyuran, A.; Wu, Z.; Loos, H.; Hall, G. E.; Suits, A. G. *Phys. Rev. Lett.* **2004**, *92*, 83002.

JP8002036